OFDM performance with odd-even quantisation

By Sirma sirma

OFDM Performance with Odd-Even Quantisation in Cartesian ΔΣ Upconverters

Sirmayanti Sirmayanti[1,2], Vandana Bassoo[3], Horace King[1], Mike Faulkner[1]

[1]School of Engineering and Science, Victoria University, Melbourne, Australia

[2]Telecommunication Engineering Study Program, the State Polytechnic of Ujung Pandang, Indonesia

[3]School of Innovative Technologies and Engineering, University of Technology, Mauritius

E-mail: {sirmayanti.sirmayanti} @live.vu.edu.au

Abstract— This paper studies the odd-quantisation technique when subjected to OFDM input signals in a Cartesian Delta Sigma (ΔΣ) upconverter. The results will be compared to the even-quantisation method of [9] to establish whether there is an improvement in performance. The overall performance of the odd-quantisation scheme has about 5dB reduced adjacent channel power (ACP) compared to the even-quantisation scheme. The smaller first quantisation step results in lower quantisation noise for small signals, leading to a lower noise floor. When the signal is frequency offset, a number of distortions become visible in the spectrum. The third harmonic is the biggest distortion contributor followed by the image. Interestingly, the overall better noise performance of the odd-quantisation scheme does not improve the distortion spectra. Best performance occurs when frequency offsetting is avoided.

I. INTRODUCTION

Currently, the communication connectivity through a wireless device plays an essential role in daily life. The rapidly developing technology of wireless transmitters such as for WLAN, mobile 3G & 4G, and public digital broadcasting will require more power efficiency, good linearity, high data rate and high bandwidth. Switch mode power amplifiers (SMPAs) have high efficiency but the linearity is very critical [1,2]. Using a pulse train for driving SMPAs with pulse width and pulse position modulation (PWM/PPM) in Cartesian ΔΣ is effective for linearity requirement [3,4]. Orthogonal Frequency Division Multiplexing (OFDM) nowadays can support high data rate communications in multi-carrier systems. However, OFDM suffers from high-peak-to-average power ratio (PAPR) that will limit the energy efficiency [5]. Therefore, for wireless connectivity, in order to obtain higher data rates, directed towards maintaining spectral efficiency, performance linearity and wide bandwidth become very critical.

All nonlinear PA classes can be operated with a switching input waveform (e.g. class D and E), resulting in SMPA for a future generation of wireless base stations. This is a potential method towards high efficiency linear radio frequency of power amplifiers (RF-PAs) which has been proposed [2]. The important technique in SMPA architecture is PWM/PPM which can be used to generate an RF signal with any amplitude and phase. PWM/PPM signals are usually quantized in both amplitude and phase. The amplitude and phase of the RF signals are controlled by the pulse width and pulse position of the switched mode output respectively. Normally, baseband signals are generated in Cartesian format. Therefore, these signals must be converted to Polar format to generate PWM/PPM signals.

The authors in [3,6] developed a Cartesian ΔΣ system to generate a binary signal with an appropriate pulse width and pulse position for driving an SMPA. ΔΣ techniques was used to shape the noise away from the band of interest. They operate by subtracting the current quantised error signal from the subsequent sample [7]. The Cartesian ΔΣ technique shown in Fig.1 was used to suppress the quantisation noise but the 'Polar to PWM/PPM' block can generate unwanted spectral components when the carrier frequency of the transmitted signal is offset from its nominal frequency [8,9].
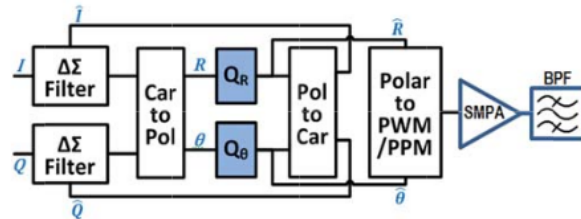

Fig. 1. Cartesian ΔΣ Upconverters. Q_R and Q_θ quantise the amplitude and phase in odd-quantisation scheme.

A novel all digital approach with a quantisation technique to generate a pulse train for driving an SMPA in the Cartesian ΔΣ system was proposed in [9]. The proposed quantiser used an even-quantisation technique where the three-level-waveform forming the output is based on pulses with an even number of clock periods. The quantised amplitudes, $\hat{R}$, of the RF signal are calculated by changing the pulsewidths in increments of two clock periods. However, this leads to a potential coarse quantisation at low signal levels as the minimum pulsewidth in the even-quantisation scheme is two clock periods.

This paper offers an alternative approach to the even-quantisation of [9] using a new scheme of odd-quantisation. Odd-quantisation was proposed to reduce the possible pulsewidths by one clock period while maintaining a constant phase reference. The acceptable pulsewidths become (0, 1, 3, 5 …) for the odd-quantisation compared to the (0, 2, 4, 6 …) values for the even-quantisation. In both cases the phase reference does not change with the pulsewidth, allowing separate quantisers for amplitude and phase.

In the following, Cartesian ΔΣ upconverter with odd-quantisation will be considered when applied to OFDM. It should be noted that most of today's modulation schemes have large signal dynamics. OFDM and Code Division Multiple Access (CDMA) are often modeled with a Rayleigh amplitude distribution. The signals must be backed off so that the

electronics can handle the peak powers. The result is that there is an increased probability of low signal levels in the $\Delta\Sigma$ modulator. Ideally, therefore, the quantisation levels should also be concentrated at the low signal levels.

The contribution of this paper is the evaluation of the adjacent channel interference caused by the quantisation process in the $\Delta\Sigma$ architecture. We show that both even-quantisation and odd-quantisation schemes produce the same distortion products that increase with frequency offset. On the other hand, when the input signal is backed-off (power control), the noise problem is reduced with the odd-quantisation.

The paper is organized as follows. Section I is the introduction. Section II presents the details of the new odd-quantisation scheme. Section III and section IV give the simulation setup and results of the OFDM test signal for both even-quantisation and odd-quantisation schemes. Finally, we draw a conclusion in section V.

II. ODD QUANTISATION SCHEME

$\Delta\Sigma$ filtering is achieved through the processes oversampling and noise shaping. Oversampling reduces the noise power spectral density (PSD) when the noise is spread over a wider bandwidth. As expected, increasing the baseband (BB) oversampling rate (OSR_{BB}) will decrease the in-band noise proportional to $\frac{1}{OSR}$ [7]. The oversampling ratio of the baseband is given by

$$OSR_{BB} = \frac{f_s}{f_B} \tag{1}$$

where f_B is the maximum signal bandwidth and f_s is the sampling frequency. The quantisation error is also noise shaped using feedback in the $\Delta\Sigma$ filter. The noise transfer function (NTF) for a lowpass 2nd order $\Delta\Sigma$ (Fig. 2) is given by:
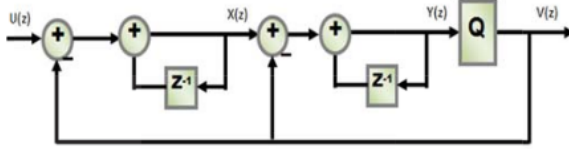
$$NTF = (1 - z^{-1})^2 \tag{2}$$

Fig. 2. Mod-2 Lowpass $\Delta\Sigma$.

The comparison between even-quantisation [9] and the new odd-quantisation schemes are now discussed. The new quantisation scheme affects the Q_R and Q_θ blocks and the PWM generation block 'Polar to PWM/PPM' of Fig.1.

The PWM/PPM process requires the digital clock (f_{clock}) to oversample the nominal RF carrier frequency of the signal output (f_c) by a factor of OSR_{RF}. The OSR_{RF} is given by

$$OSR_{RF} = \frac{f_{clock}}{f_c} \tag{3}$$

The phase is therefore uniformly quantised into N_P ($=OSR_{RF}$) increments over the range 0 to 2π. The quantised phase, $\hat{\theta}$, is determined by the pulse position. The phase reference is taken from the middle of the pulse and is 0 degrees for even pulsewidths. However the reference for odd pulsewidths is given by

$$\theta_{ref} = \frac{2\pi/N_P}{2} \tag{4}$$

The quantised amplitude, $\hat{R}$, is determined by the pulsewidth as shown in Fig. 3. The top trace shows the maximum amplitude condition for $OSR_{RF}=8$ and has a pulsewidth of four clock periods. The output is a full square wave, and after bandpass filtering produces the sinusoidal output. The bottom trace shows a reduced amplitude sinewave with a pulsewidth of three clock periods. The phase reference for the even and odd pulsewidth conditions is clearly shown.
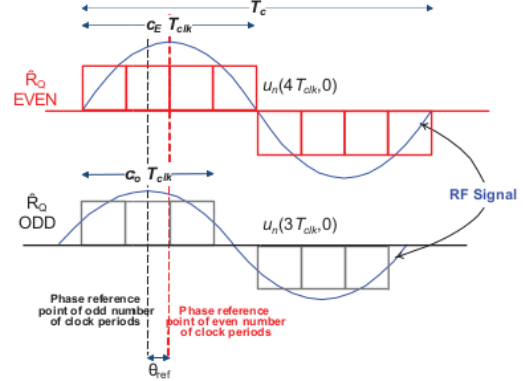
Fig. 3. Calculation for $\hat{R}$ with the even-odd number of clock periods for $OSR_{RF}=8$.

If the quantised amplitudes $\hat{R}$ are confined to all the even pulsewidths, then the phase reference does not change and so amplitude quantisation and phase quantisation are independent one dimensional operations; similarly, if the quantisation amplitudes are confined to all the odd pulsewidths. When both odd and even pulsewidths are allowed a change in amplitude can cause a change in phase (Amplitude Modulation (AM) to Phase Modulation (PM) conversion) and so joint amplitude and phase quantisation must be applied. This is a two-dimensional operation and leads to a great increase in quantiser complexity.

Fig. 4 shows the even-quantisation and the odd-quantisation in the Polar plane. The radius of the circles is set by $\hat{R}$. The radial lines show the quantised phase, $\hat{\theta}$. The even-quantised points of $Q_E[\hat{R}, \hat{\theta}]$ are illustrated by red dots. The odd-quantised points of $Q_O[\hat{R}, \hat{\theta}]$ are illustrated by the black crosses. $\hat{R}$ and $\hat{\theta}$ are the quantised values of $[R,]$ corresponding to the I and Q output of the $\Delta\Sigma$ filters. The dashed circles between each of circles (red is for even-Polar, and black is for odd-Polar) are the threshold levels for the amplitude quantiser ($\hat{L}_R$). The phase threshold levels, ($\hat{L}_\theta$), are measured midway between two phase increments, and are shown as dashed lines.

The quantised phase is based on the odd-Polar plane, as shown in Fig. 4 (below), given by

$$\hat{\theta} = (p_p + 0.5)\frac{2\pi}{N_P} \tag{5}$$

The threshold for the quantised phase is calculated by equation

$$L_\theta(p_p, p_p + 1) = p_p\frac{2\pi}{N_P} \tag{6}$$

The amplitude levels are calculated by evaluating the fundamental spectral component of the three-level waveform, $u_n(p_o, p_p)$, with amplitudes 1, 0, and -1. p_o is the pulsewidth

corresponding to the c_O clock cycles (c_O is for odd) or c_E clock cycles (c_E is for even). p_p is the pulse position and refers to the time delay or advance. $p_p = (0, \dots (N_P\text{-}1))$ and represents the PPM delay in clock periods.
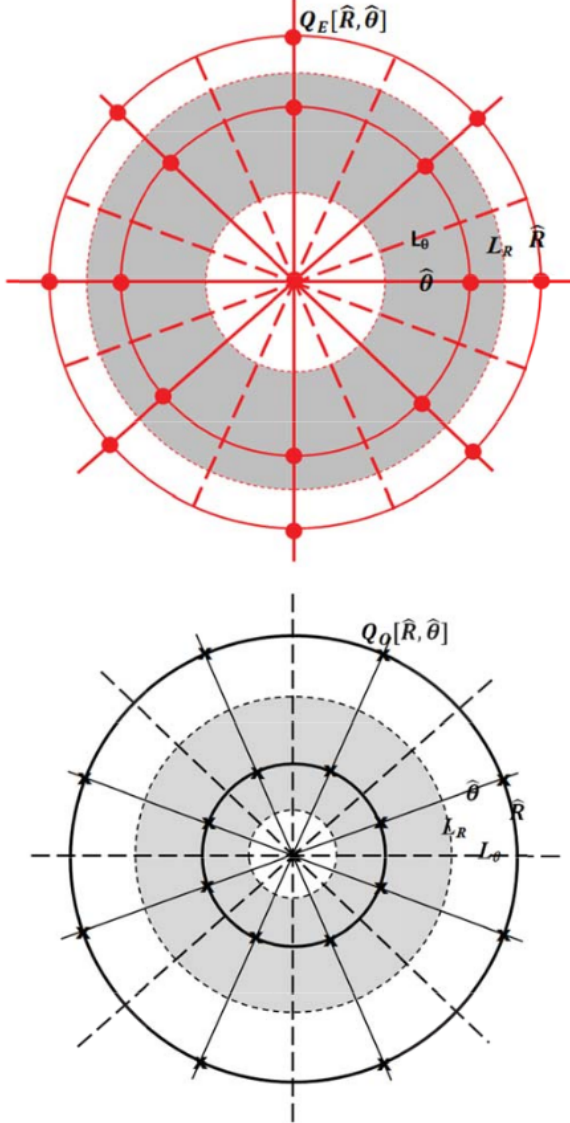

Fig. 4. The even-quantisation (top) and the odd-quantisation (below) Polar plane scale for OSR_{RF}=8.

Since $u_n(p_o, p_p)$ is a repeating waveform, the amplitude of the spectral component can be generated from one period only using the Fourier series. Here, we use a highly oversampled version of $u_n(p_o, p_p)$ to get the same result from a discrete Fourier transform (DFT).

$$U_k(p_o, p_p) = \frac{1}{K} DFT(u_n(p_o, p_p)) \quad (7)$$

where K is the fast Fourier transform (FFT) size. The amplitude of the fundamental of the pulse wave occurs in the first frequency bin, k=1

$$\hat{R}_Q\left(\frac{p_o}{2}\right) = 2[|U_{k=1}(p_o, p_p)|], \quad (8)$$

$\left(\frac{p_o}{2}\right)$ is the index for the different pulsewidths corresponding to the odd pulsewidth $\left(0, \frac{1}{OSR_{RF}}, \frac{3}{OSR_{RF}} \dots \frac{N_P-1}{OSR_{RF}}\right)\frac{1}{f_c}$.

The amplitude threshold levels are given by the midpoint of two amplitude quantised levels,

$$L_R\left(\frac{p_o}{2}, \frac{p_o}{2} + 1\right) = \frac{R\left(\frac{p_o}{2}\right) + R\left(\frac{p_o}{2} + 1\right)}{2}, \quad (9)$$

where the index of $\frac{p_o}{2}$ is selected in ascending order.

After quantisation, then the 'Polar to PWM/PPM' block is used to convert the quantised signals, $[\hat{R}, \hat{\theta}]$, in Polar representation to RF using PWM and PPM schemes. The location of the pulse position of the PPM process is determined using the quantised phase, $\hat{\theta}$, which is the output from Q_θ block. A change in position depends on a change of $\hat{\theta}$ where the pulse edges must occur on the digital timing grid. The output of Q_R block, $\hat{R}$, determines the duration of the PWM process.
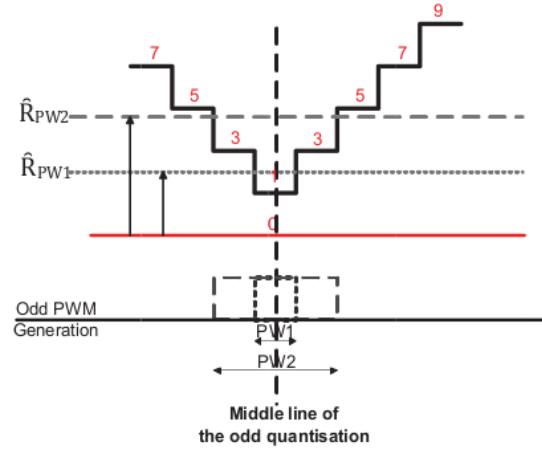

Fig. 5. Odd PWM generation.

Fig. 5 illustrates the PWM generation of odd quantised signals using a stepped triangle wave. It shows two examples of quantised amplitudes: $\hat{R}_{PW1}$ and $\hat{R}_{PW2}$. The output pulsewidths, $PW1$ and $PW2$, are defined by the crossing points of the line $\hat{R}_{PW1}$ and $\hat{R}_{PW2}$ respectively and the stepped triangular waveform signal. The pulsewidth must change with two sample increments to decouple the amplitude response from the phase response. The pulsewidth then maintains symmetry about its midpoint.

III. TEST SIGNAL CHARACTERISTICS OF OFDM

Fig. 6 shows the simulation model for test signal OFDM into Cartesian $\Delta\Sigma$ upconverters. The OFDM bandwidth (B) was set at $\frac{f_c}{64}$ with f_c=1024 MHz which equivalent to a B_{ofdm} of 16 MHz (applicable bandwidth to WLAN). The sampling frequency (f_s) of the $\Delta\Sigma$ is related to the nominal carrier frequency f_c.

$$f_s = \frac{f_c}{m} \quad (10)$$

where the index m is the number of carrier periods between each output sample of the $\Delta\Sigma$, (m=n/2, where n is an integer).
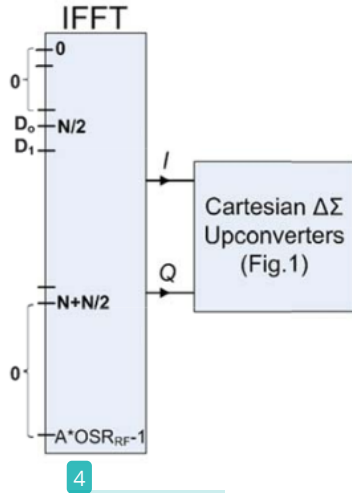
Fig. 6. OFDM as input the *I* and *Q* signal to Cartesian ΔΣ upconverters for an offset carrier.

Fig. 7. Spectrum plot of even-quantisation and odd-quantisation in Cartesian ΔΣ upconverter with offset OFDM signal.

When $n=1$ and $m=1/2$, the pulse width and position is updated every half period of the carrier, which is the highest update rate. In this work we use $m=1$ ($n=2$) and update every period. If Δf is the bin frequency spacing between the active tones (A) of subcarriers, therefore B_{ofdm} is equal to $A*\Delta f$. N is the nominal number of subcarriers in the channel bandwidth, including the null sub-carriers forming the guard band between adjacent channels. The simulation parameters are summarized in Table I.

TABLE I
SIMULATION PARAMETERS

Parameter	Value
Modulated Signal	QPSK, OFDM
Frequency carrier, f_c	1024 MHz
OSR_{BB}	64
Oversampling ratio (OSR_{RF})	16
N	20
A	16
Δf	1 MHz
Offset frequency	20 MHz, guard band $0.25 B_{ofdm}$

IV. SIMULATION RESULTS

A spectrum plot of a pulse waveform with an RF carrier OSR_{RF} of 16 and an input signal level, $u= -7$ dB (with respect to $u_{rms}= 1$) obtained at the output of the Cartesian ΔΣ upconverter is shown in Fig. 7. The adjacent channels and the nominal position of the carrier are drawn on the figure to facilitate the understanding of the plot. The signal is present in channel 1. The image is present in channel -1 and the third harmonic is situated in channel 3 with the highest noise. The noise is lowest in channel 0 as the NTF of the ΔΣ operates from f_c and maximum attenuation of quantisation noise occurs around that region (ΔΣ-filters with MOD2).

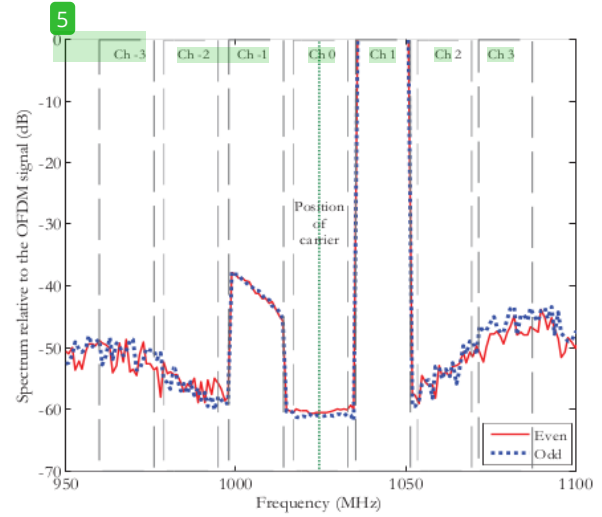The out-of-band distortions for both even-quantisation and odd-quantisation schemes are compared by calculating their adjacent channel powers (ACPs). The desired signal was shifted one channel to the right to examine the resultant spectral images. The ACPs which are defined as the noise power in the adjacent channel divided by the signal power were calculated. The noise power includes quantisation noise as well as distortion arising from PPM.
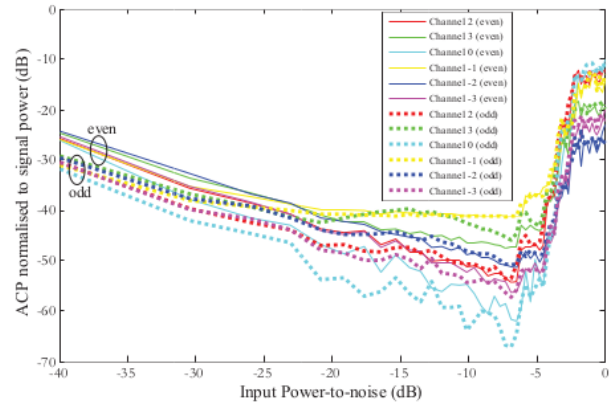

Fig. 8, Cartesian ΔΣ with even-quantisation and odd-quantisation scheme (ACP in adjacent channel vs. input level).

Fig. 8 shows a plot of input level (dB) against ACP (dB) for the six adjacent channels obtained after simulating the Cartesian ΔΣ scheme. The shape of the curves indicates -7dB is the optimum input signal level for best SNR. As shown in the figure, the odd-quantisation has reduced ACP compared to even-quantisation for most input signal levels; only at large signal levels is the improvement less obvious. In channel 2, the odd-quantisation scheme has at least 4.83 dB less ACP than the even-quantisation scheme. In channel 0, the odd-quantisation scheme has at least 5.57 dB less ACP than the even-quantisation scheme. Again, it can be observed that

channel 3 (Fig.7) which represents the third harmonic has the highest noise. Channel -1 representing the image has the second highest noise. Channel 0 has lower noise than channel 2 as channel 0 is centered at f_c. This plot further validates the conclusions drawn from Fig. 7.

V. CONCLUSION

This paper compares even-quantisation and odd-quantisation schemes for Cartesian $\Delta\Sigma$ upconverters. OFDM is used as the input signal. The characteristics of the input test signals and the OSR for both schemes are kept the same. The overall performance of the even-quantisation scheme is worse than the odd-quantisation scheme as the even-quantisation structure has an inherently higher noise floor. It can be observed that the third harmonic is the biggest noise contributor followed by the image. Interestingly, the overall better performances of the odd-quantisation scheme occur at lower input signal levels. These levels benefit from the lower first quantisation step of the odd-quantisation scheme. The benefit is lost when the input signal level rises to within about 7dB of the optimum signal level. The image and third order distortions dominate the performance at large signal levels and make signal tuning by using frequency offsetting at baseband a non-attractive proposition. The type of quantisation does not improve this aspect of the output spectrum. Tuning by changing the sample rate would obviate the need for offsetting and so avoid the problem.

VI. REFERENCES

[1]   P. Lavrador, T. Cunha, P. Cabral, and J. Pedro, "The linearity-efficiency compromise", IEEE Microw Mag., Vol.11, No. 5, pp. 44-48, Aug. 2010.

[2]   H. Sjoland, et al, "Switched Mode Transmitter Architectures," in Analog Circuit Design Smart Data Converters, Filters on Chip, Multimode Transmitters, A.H.M Van Roermund, Ed. Netherlands: Springer, pp. 325-342, 2009.

[3]   V. Bassoo et.al, "A potential transmitter architecture for future generation green wireless base station", EURASIP Journal on Wireless Com. & Net. Article ID 821846, 8 pages, 2009.

[4]   B. T. Thiel, et al, "System Architecture of an All-Digital GHz Transmitter using Pulse-Width/Position-Modulation for Switching-Mode PAs," Asia Pacific Microwave Conference (APMC), pp.2340–2343, Dec 2009.

[5]   R. V. Nee and R. Prasad, "OFDM for wireless multimedia communications", Artech House Publisher, 2000.

[6]   V. Bassoo and M. Faulkner, "Sigma Delta Digital Drive Signals for Switch mode Power Amplifiers", Electronic Letters, Vol. 44, Issue 22, pp. 1299-1300, Oct 2008.

[7]   R. Schreier and G.C. Temes, "Understanding delta-sigma data converters", Wiley Press, 2004.

[8]   S. Sirmayanti, et.al., "Sigma Delta ($\Sigma\Delta$) Architecture Integration with Digital Pre-distortion to enhance Optimal Switch Mode Power Amplification (OSMPA) in FEMTO cell Transceiver Design", in Proc. IEEE 8th ICICS, Singapore, pp. 1-4, Dec 2011.

[9]   V. Bassoo, Linton L., Faulkner M., 'Analysis of distortion in pulse modulation converters for switching radio frequency power amplifiers' IET Microwave. Antennas Propag. Vol. 4, Issue. 12, pp. 2088-2096, Dec 2010.

[10] B. Razavi, "RF microelectronics", Prentice Hall Ptr, 1998.

OFDM performance with odd-even quantisation

delta-sigma (ΔΣ) upconverters", 2013 Africon, 2013
Crossref

9   diglib.tugraz.at
    Internet   9 words — < 1%

10 pure.tue.nl
    Internet   8 words — < 1%

11 www.slideshare.net
    Internet   8 words — < 1%

12 Sirmayanti Sirmayanti, Mike Faulkner.
    "ΣΔ modulator for digital wireless   6 words — < 1%
    architecture: A review", 2014 Makassar International
    Conference on Electrical Engineering and Informatics (MICEEI),
    2014
    Crossref

EXCLUDE QUOTES   OFF   EXCLUDE SOURCES   OFF
EXCLUDE BIBLIOGRAPHY ON   EXCLUDE MATCHES   OFF